Gilbert-like damping caused by time retardation in atomistic magnetization dynamics

Danny Thonig,[1,*] Jürgen Henk,[2] and Olle Eriksson[1]
[1]*Department of Physics and Astronomy, Material Theory, University Uppsala, S-75120 Uppsala, Sweden*
[2]*Institut für Physik, Martin-Luther-Universität Halle-Wittenberg, D-06099 Halle (Saale), Germany*
(Received 26 May 2015; revised manuscript received 27 June 2015; published 4 September 2015)

Gilbert-like damping in magnetization dynamics is commonly attributed to the interplay of the spin, the electron, and the phonon reservoirs. Spatial correlations within the spin reservoir itself, for example magnons, mediate damping as well. We show theoretically that temporal correlations within the spin reservoir cause a similar effect. We investigate the role of time retardation in the atomistic Landau-Lifshitz-Gilbert equation using two different retardation kernels. Although viscous damping is explicitly excluded, we find both analytically and numerically that damping and higher-order effects emerge due to time retardation. Thus, our results establish a mechanism for damping and inertia in magnetic systems.

DOI: 10.1103/PhysRevB.92.104403 PACS number(s): 75.10.Hk, 75.40.Mg, 75.78.−n

I. INTRODUCTION

New developments in spintronics are often related to switching magnetic moments [1–4]. The efficiency of the switching process can be manipulated either by external magnetic fields or by magnetic properties of the material under consideration, e.g., by selecting compounds with strong spin-orbit coupling [5,6] or with large dissipation of energy and angular momentum. Both influence the effective precession as well as the Gilbert dissipation [7] and, thus, the dynamics of the magnetic moments. In particular, the Gilbert damping is of utmost importance since it determines the velocity of the switching as well as the thermal stability of the magnetic system.

Dissipation in a magnetic system is ascribed to coupling of the spin reservoir to the electron or the phonon reservoirs (illustrated schematically in Fig. 1). The breathing Fermi surface model [8] attributes the Gilbert damping α to the coupling of the electron and the phonon reservoir. Here, deviations from the collinear ground state, with magnetization along an easy axis, produce an out-of-equilibrium electronic ground state; the relaxation of this excited state back to an equilibrium state requires energy dissipation and takes place either between the electron and spin reservoirs (with strength α) or between the electron and phonon reservoirs (with relaxation time $\tau_{\mathrm{ep}} = \hbar/\Sigma_{\mathrm{ep}}$). It has been shown by Gilmore *et al.* [9] that the lower the coupling energy Σ_{ep}, the higher the dissipation of energy and angular momentum in the magnetic system. This trend has been corroborated within a linear-response model by Ebert *et al.*: in Refs. [10] and [11], a decrease of the Gilbert damping with the phonon temperature has been established and, furthermore, the dominance of the phonon contribution is analyzed. Steiauf and Fähnle point out a nonlocality as well as an anisotropy of the damping in space and with respect to the direction of the magnetic moments [12,13]. In addition, a significant influence of the electron and spin temperatures on the damping has been established [14].

Besides electron-phonon coupling, other damping mechanisms are conceivable; for example, a direct coupling of the phonon and the spin reservoirs [15], a spin-orbit-influenced electron gas in nonequilibrium [16], as well as damping within the spin reservoir itself. The latter mechanism, in particular, is related to the exchange of angular momentum between magnetic quasiparticles, as has been reported for magnon-magnon scattering [17] or for magnon-skyrmion scattering [18,19]. A mismatch between ferromagnetic resonance and field-driven domain wall dynamics has been resolved by nonlocal damping within the spin reservoir [20].

The above discussion provides examples of "magnetic damping" attributed to *spatial* correlation among the magnetic moments. This immediately raises the question of whether *temporal* correlation could result in damping as well; if so, such a mechanism should be called time-retarded damping. In this paper, we point out this possibility.

Retardation effects have been investigated by Bose [21] for mesoscopic magnetic systems. Taking into account retardation effects in both time and space in the equation of motion led to an increase of the effective Gilbert damping and of the Larmor frequency. This has been attributed to a coupling of the magnetic configuration at time t to that at $t' < t$ and to nonlocal dissipation. The latter effect has been confirmed by experiments [22] and by theory [14,15]. Predictions of magnetic configurations on the atomic level and, consequently, a discussion of the role of intrinsic magnetic properties—e.g., exchange or magnetocrystalline anisotropy—are hardly possible in a mesoscopic model. This calls for a study of time retardation on the atomic scale.

In this paper, we report on an investigation of the time-retarded equation of motion on the atomic scale. The approach is applied to a macrospin system as well as to the bulk ferromagnets Fe and Co. By studying the parameter space of the retardation kernels—both analytically and numerically—we show that Gilbert-like damping is determined by the effective magnetic field at time t', which obviously depends on the exchange coupling and on the magnetocrystalline anisotropy. We also find a sizable influence of the correlation duration τ_{s}.

The paper is organized as follows. In Sec. II, we introduce time retardation in the Landau-Lifshitz-Gilbert equation as well as the retardation kernels. In addition, we provide details of the numerical calculations. We proceed with applications to a macrospin (Sec. III A) and to atomic systems (bulk Fe and Co; Sec. III B). Conclusions are given in Sec. IV.

*danny.thonig@physics.uu.se

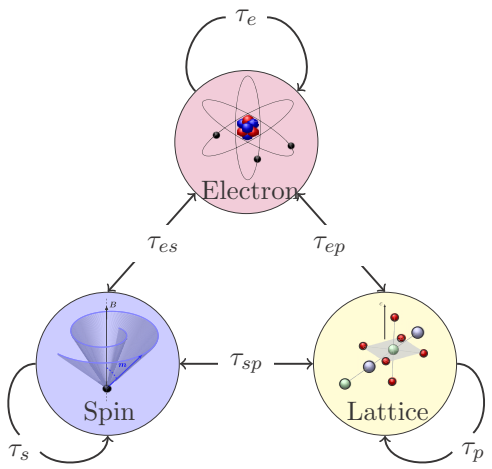

FIG. 1. (Color online) Interplay between and within the electron, the spin, and the phonon reservoir (schematic). The associated relaxation times τ are indicated.

II. THEORETICAL ASPECTS

The time-retarded equation of motion for a mesoscopic magnetic moment $\boldsymbol{M}$ at position $\boldsymbol{r}$ and at time t reads [23,24]

$$\frac{\partial \boldsymbol{M}(\boldsymbol{r},t)}{\partial t} = \int_0^t dt' \int d^3r' \, \boldsymbol{\Gamma}(\boldsymbol{r},t;\boldsymbol{r}',t')\boldsymbol{M}(\boldsymbol{r}',t') \times\left[-\gamma \boldsymbol{B}(\boldsymbol{r}',t') + \frac{\alpha}{M_s}\frac{\partial \boldsymbol{M}(\boldsymbol{r}',t')}{\partial t'}\right], \quad (1)$$

where M_s is the saturation magnetization, α is the damping constant, and γ is the gyromagnetic ratio. In this equation, magnetic "velocities" are integrated from the initial time $t' = 0$ to time t and over all positions $\boldsymbol{r}'$, weighted with the retardation kernel $\boldsymbol{\Gamma}(\boldsymbol{r},t;\boldsymbol{r}',t')$. More precisely, the velocity $\partial \boldsymbol{M}(\boldsymbol{r},t)/\partial t$ of the magnetic moment at $\boldsymbol{r}$ and t is determined by the torque of the magnetic moment with respect to the effective field $\boldsymbol{B}(\boldsymbol{r}',t')$ and the dissipation field

$$\boldsymbol{B}^{\mathrm{diss}}(\boldsymbol{r}',t') \equiv \frac{\alpha}{M_s}\frac{\partial \boldsymbol{M}(\boldsymbol{r}',t')}{\partial t'}. \quad (2)$$

The retardation kernel $\boldsymbol{\Gamma}(\boldsymbol{r},t;\boldsymbol{r}',t')$ models the space-time correlation between the magnetic moments. For example, in Ref. [25], time retardation similar to Eq. (1) was used for the dissipation field only to derive the magnetic inertia in the equation of motion. In this paper, we address solely time retardation; thus $\boldsymbol{\Gamma}(\boldsymbol{r},t;\boldsymbol{r}',t')$ is approximated by $\boldsymbol{\Gamma}(t,t')$. This implies that the space retardation is completely given by the effective field $\boldsymbol{B}(\boldsymbol{r},t')$.

To map the mesoscopic equation (1) onto the atomistic level—in other words, replacing the continuous domain by a discretized one—one has to be aware that there is no one-to-one correspondence with the mesoscopic model, in contrast to the conventional Landau-Lifshitz-Gilbert (LLG) equation. By requiring normalized atomic magnetic moments ($|\boldsymbol{m}_i| = m_s$, where i is a site index), the condition $\boldsymbol{m}_i(t) \times \boldsymbol{m}_i(t') = 0$ cannot be guaranteed by Eq. (1). This problem is overcome by introducing a retardation field $\boldsymbol{B}^{\mathrm{ret}}$ in the atomistic magnetization dynamics. The modified atomistic LLG equation then reads

$$\frac{\partial \boldsymbol{m}_i(t)}{\partial t} = \boldsymbol{m}_i(t) \times \int_0^t dt' \boldsymbol{\Gamma}_i(t,t')\left[-\gamma \boldsymbol{B}_i(t') + \frac{\alpha}{m_s}\frac{\partial \boldsymbol{m}_i(t')}{\partial t'}\right], \quad (3)$$

which fulfills the above normalization condition. Here, $\boldsymbol{\Gamma}_i$ is assumed local at site i. The retardation field is given by

$$\boldsymbol{B}_i^{\mathrm{ret}}(t) = \int_0^t dt' \boldsymbol{\Gamma}_i(t,t')\left[\boldsymbol{B}_i(t') - \frac{\alpha}{\gamma m_s}\frac{\partial \boldsymbol{m}_i(t')}{\partial t'}\right]. \quad (4)$$

In the following, the retardation kernel $\boldsymbol{\Gamma}(t,t')$ depends on the duration $t - t'$. Hence, the obtained equation of motion (3) is of Cummins type [26]: mass and damping are due to the convolution integral and are included in the operator[1]

$$\boldsymbol{\Gamma}(t) \approx -\frac{1}{\pi}\int_0^\infty d\omega m(\omega) \times\left[\frac{\boldsymbol{\alpha}^{\mathrm{ret}}(\omega)}{m_s}\cos(\omega t) + \frac{\boldsymbol{\iota}^{\mathrm{ret}}(\omega)}{m_s}\sin(\omega t)\right]. \quad (5)$$

Here, $m(\omega)$, $\boldsymbol{\alpha}^{\mathrm{ret}}(\omega)$, and $\boldsymbol{\iota}^{\mathrm{ret}}(\omega)$ are the Fourier-transformed magnetic moment, the retarded damping tensor, and the retarded moment-of-inertia tensor, respectively. Note that $\boldsymbol{\alpha}^{\mathrm{ret}}$ and $\boldsymbol{\iota}^{\mathrm{ret}}$ are defined differently than $\boldsymbol{\alpha}$ in Ref. [7] and $\boldsymbol{\iota}$ in Refs. [27] and [28]. Equation (5) establishes a time dependence of the damping and of the inertia; both are approximated by a functional $\alpha = \alpha[\boldsymbol{m}]$ in Ref. [15].

Since the forms of both $\boldsymbol{\alpha}^{\mathrm{ret}}(\omega)$ and $\boldsymbol{\iota}^{\mathrm{ret}}(\omega)$ are unknown, the retardation kernel $\boldsymbol{\Gamma}(t - t')$ has to be approximated. In this paper, we focus on two kernels. The first kernel describes an exponential decay in time,

$$\boldsymbol{\Gamma}^{\mathrm{exp}}(t - t') \equiv [\Gamma_0\delta(t' - t) + \Gamma_1 e^{-(t-t')/\tau_s}]\mathbb{1}_{3\times3}. \quad (6)$$

The correlation time τ_s defines—loosely speaking—the "strength of memory." The strength of the retardation is given by Γ_0 and Γ_1. Γ_0 is fixed by $\Gamma_0 = 1/\delta t$, where δt is the step width in the numerical integration. Equation (3) can be rewritten in LLG form, but with the additional retardation field $\boldsymbol{B}^{\mathrm{ret}}$,

$$\frac{\partial \boldsymbol{m}_i}{\partial t} = \boldsymbol{m}_i \times \left(-\gamma \boldsymbol{B}_i + \frac{\alpha}{m_s}\frac{\partial \boldsymbol{m}_i}{\partial t} - \gamma \boldsymbol{B}_i^{\mathrm{ret}}\right). \quad (7)$$

$\Gamma_1 = 0$ in Eq. (6) makes Eq. (7) equivalent with the conventional LLG equation. To include higher exponential orders in τ_s, we consider also a second kernel, a Gaussian with amplitude Γ_0,

$$\boldsymbol{\Gamma}^{\mathrm{Gauss}}(t - t') = \frac{\Gamma_0}{\sqrt{2\pi}\tau_s}e^{-(t-t')^2/2\tau_s^2}\mathbb{1}_{3\times3}. \quad (8)$$

In what follows, the retardation kernel is assumed to be site independent and isotropic because we focus on collinear magnetic states. Furthermore, we explicitly neglect the Gilbert-type dissipation in Eq. (3) by setting $\alpha \equiv 0$, in order to explore other mechanisms of damping.

[1]Equation (5) is obtained by Fourier transforming the Landau-Lifshitz-Gilbert equation and comparing it with Eq. (14.20) of Ref. [26].

The effective field in Eq. (3) is given by $\boldsymbol{B}_i = {}^{-\partial \hat{H}}/_{\partial \boldsymbol{m}_i}$, in which the magnetic Hamiltonian

$$\hat{H} = -\sum_{ij} J_{ij} \boldsymbol{m}_i \cdot \boldsymbol{m}_j + \sum_i K_i (\boldsymbol{m}_i \cdot \boldsymbol{e})^2 - \mu_B \boldsymbol{B}^{\text{ext}} \cdot \sum_i \boldsymbol{m}_i \tag{9}$$

consists of three terms. The first term is the Heisenberg exchange that couples two atomic magnetic moments at sites i and j by the strength J_{ij}; the second term is the uniaxial magnetocrystalline anisotropy with the uniaxial direction $\boldsymbol{e}$ and the anisotropy constant K_i. In this paper, the set of $\{J_{ij}\}$ is calculated for bulk Fe and Co using the Lichtenstein formula [29] within the framework of relativistic multiple-scattering theory (Korringa-Kohn Rostoker method) [30,31]. The last term in Eq. (9) is a Zeeman term that couples the magnetic moments to an homogeneous external magnetic field $\boldsymbol{B}^{\text{ext}}$.

The semiclassical Landau-Lifshitz approach on the atomistic scale has been successfully applied in the last decade [32–34] and was derived in Refs. [35] and [36] from quantum-mechanical principles via the adiabatic approximation. In the aforementioned papers, it was shown that the semiclassical Landau-Lifshitz-Gilbert equation provides reasonably accurate results even in the case of an atomistic model; however, it goes without saying that for precise accounting of magnetic phenomena on the atomic level, corresponding quantum-mechanical calculations should be carried out. Note that the adiabatic approach is reasonable since the time scales in the atomistic model (cf. Fig. 1)—attoseconds for the electron reservoir and picoseconds for the spin reservoir—are still separable. However, Wieser *et al.* [37,38] point out a discrepancy between the atomistic semiclassical and the quantum-mechanical model if the magnetic Hamiltonian contains terms that are quadratic in the magnetic moments $\boldsymbol{m}_i$; the latter is the case for a uniaxial magnetocrystalline anisotropy.

The retarded LLG equation is solved for a set of magnetic moments $\{\boldsymbol{m}_i\}$ by an iterative partial-differential equation solver which is based on the midpoint method [39]. The iteration error is less than 1×10^{-9}. The integration is performed by the trapezoidal method, but cut at a time t' for which the retardation kernel is smaller than 1×10^{-5} fs^{-1}. For high accuracy, time steps ranging from 1×10^{-5} up to 1×10^{-4} fs are required. Our spin dynamics code[2] has been run over at least 5×10^7 time steps, allowing one to observe relaxations within 1 ps. The cluster size is $5 \times 5 \times 5$ times two atoms in the unit cell (250 atoms), which turns out to be sufficiently large for our purposes. Periodic boundary conditions [40] are applied to evaluate properly bulk properties. The convergence of the cluster size has been checked by simulations for larger clusters [up to $10 \times 10 \times 10$ (2000 atoms) for small τ_s], reproducing the same results as for the smaller clusters in a collinear and coherent state. Note that the minimal cluster size (250 atoms) is dictated by the maximal interaction distance $r_{\max}$ (here, convergence is examined up to $r_{\max} = 5 \times a$, where a is the lattice constant) and is used to achieve larger values of τ_s. The conditions of collinearity and coherence are valid since $T = 0$ K in our model.

The Fourier space of a selected magnetic moment $\boldsymbol{m}_i$ and, consequently, its precession frequency ω as well as its nutation frequency ω_n are extracted from the trajectory $\{\boldsymbol{m}_i(t)\}$ of the moment at site i by using a fast Fourier transformation based on the Danielson-Lanczos algorithm. Note that in the collinear magnetic state (macrospin state), the precession and nutation frequencies are not dependent on the site and, consequently, could be obtained from the average magnetic moment. Noncollinear magnetic states are mediated, e.g., by lower coordination in the lattice and, consequently, anisotropic effective Heisenberg exchange or by site-dependent magnetic anisotropies, resulting in retardation frequencies and damping parameters that depend on the atomic site i. This is valid for a wide range of parameter sets $\{J_{ij}\}$ and $\{K_i\}$. A damping rate R indicates how fast a magnetic moment relaxes towards the external magnetic field which is along the z axis; it is defined by the slope of the trajectory $\{m_{i,z}(t)\}$,

$$R = \frac{dm_{i,z}(t)}{dt}. \tag{10}$$

Equation (7) does not contain a stochastic field ("thermal noise") which introduces a temperature dependence [35]. For the conventional LLG equation, this field is derived from Markovian Langevin dynamics. For the retarded LLG equation, this approach is not applicable since the stochastic process would require solving a non-Markovian Langevin-like equation [41]. Hence, the results presented in the following are for zero temperature, albeit Eq. (3) can, in general, be solved at finite temperatures.

III. DISCUSSION OF RESULTS

In what follows, the initial configuration of magnetic moments is always collinear along the x axis. We apply a homogeneous external magnetic field of 10 T in the z direction. This setup is motivated by previous studies of higher-order effects in magnetization dynamics [42]. As mentioned, the Gilbert damping α in Eq. (3) is set to zero.

A. Macrospin

As a first example, we discuss the retardation for a macrospin [43], which is introduced by the "exponential" kernel in Eq. (6). For such an effective single-spin system, there is no Heisenberg exchange; thus, the dynamics of the macrospin is determined by the magnetocrystalline anisotropy, the external magnetic field, and the relative orientation between these two fields.

It is conceivable that the macrospin precesses around the effective field $\boldsymbol{B}$ if both the external magnetic field and the easy axis $\boldsymbol{e}$ (for $K < 0$) of the anisotropy field are parallel. More precisely, the precession frequency ω (Larmor frequency) is determined by the strengths of the external and the anisotropy field. Since the convolution integral "sums up" fields from

[2]Computer code CAHMD, classical atomistic Heisenberg magnetization dynamics. A computer program package for atomistic magnetization dynamics simulations. (danny.thonig@physics.uu.se, 2013) (unpublished).

time t' orientated in the z direction, the Larmor frequency increases owing to time retardation. Hence, damping in this highly symmetric field configuration shows up only if the Gilbert damping α in Eq. (3) is nonzero.

Because the dissipation field in the LLG equation is proportional to the nutation frequency ω_n of the magnetic moment, it is perpendicular to $\boldsymbol{m}$. Thus, the retardation field has to be perpendicular to $\boldsymbol{m}$ as well. This can be achieved by an anisotropy field in the x direction, for which we fix $K < 0$ with an easy axis along x. The dissipative retardation field then reads

$$\boldsymbol{B}^\mathrm{ret}(t) = K \int^t \boldsymbol{\Gamma}(t,t')[\boldsymbol{m}(t')\cdot\boldsymbol{e}]dt'\boldsymbol{e}, \tag{11}$$

with $\boldsymbol{e} = (1,0,0)$. Relaxation into the direction of the external magnetic field occurs even if $\Gamma_1 \equiv 0$, since the in-plane anisotropy field mediates a torque parallel to the external magnetic field. Consequently, if the anisotropy is larger than the external magnetic field, the precession in the yz plane dominates.

For an external field much larger than the anisotropy field, the damping will be small. The dynamics is then dominated by precession within the xy plane, expressed as

$$\boldsymbol{m} = m\begin{pmatrix}\cos(\omega t)\\ \sin(\omega t)\\ 0\end{pmatrix} \tag{12}$$

(black lines in Fig. 2). Integration of Eq. (11) for small t gives

$$\boldsymbol{B}^\mathrm{ret}(t) \approx \frac{K\Gamma_1\tau_\mathrm{s}}{\omega^2\tau_\mathrm{s}^2+1}\left(\boldsymbol{m}\cdot\boldsymbol{e} + \tau_\mathrm{s}\frac{\partial\boldsymbol{m}}{\partial t}\cdot\boldsymbol{e}\right)\boldsymbol{e} \tag{13}$$

for the kernel $\boldsymbol{\Gamma}^\mathrm{exp}$ in Eq. (6). Comparison with the nonretarded Landau-Lifshitz-Gilbert equation suggests to define a time-retarded damping constant,

$$\alpha^\mathrm{ret} \equiv \frac{K\Gamma_1\tau_\mathrm{s}^2}{\omega^2\tau_\mathrm{s}^2+1}. \tag{14}$$

This result readily illustrates the proportionality of the retarded anisotropy field and a Gilbert-like damping α^ret. Since the damping is related to the projection onto the anisotropy axis, stimulation ("negative" damping) can occur as well, which

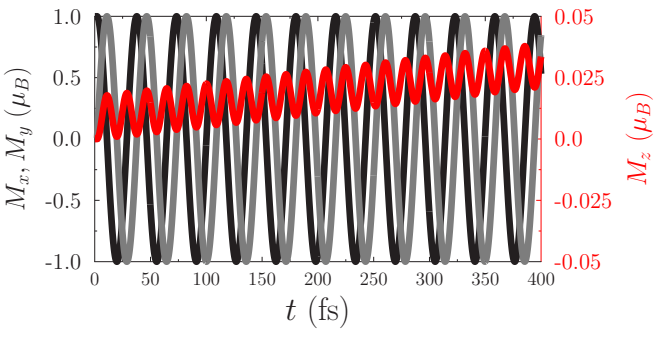

FIG. 2. (Color online) Trajectory (M_x, M_y, M_z) of a macrospin under the influence of time retardation. The in-plane components of the magnetic moment (M_x black line, M_y gray line) show precession, whereas the out-of-plane component (red line) exhibits dissipation and inertia. The retardation time and the retardation amplitude are $\tau_\mathrm{s} = 100$ as and $\Gamma_1 = 0.5\,\Gamma_0$, respectively. $m_\mathrm{s} = 1\ \mu_\mathrm{B}$ and $K = -10\ \mu$eV.

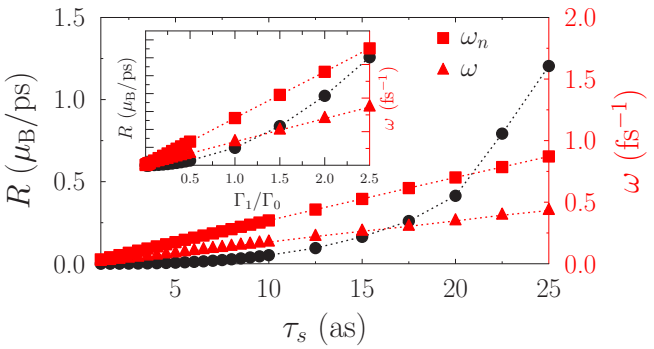

FIG. 3. (Color online) Damping rate R (black circles), precession frequency ω (red triangles), and nutation frequency ω_n (red squares) for a macrospin vs retardation time τ_s. Parameters as in Fig. 2. Inset: The damping rate R (black circles), precession frequency ω (red triangles), and nutation frequency ω_n (red squares) of a macrospin vs correlation strength Γ_1/Γ_0. The retardation time τ_s equals 2 as. The ordinate has the same scale as in the main figure. Lines are added to guide the eye.

can be attributed to the inertia of the magnetic moment (cf. the oscillation in the red line in Fig. 2).

Stimulation of the magnetic moment stems from precession that is caused by the in-plane uniaxial anisotropy field and superimposes with the precession around the external magnetic field. It governs the oscillations of the magnetic-moment-on-external-magnetic-field projection, where the oscillation amplitude depends on the anisotropy parameter K (not shown here); and thus, the superposition of both fields leading to a larger nutation frequency ω_n than the frequency ω coming from the external magnetic field only (red lines in Fig. 3). These oscillations "survive" for the time-retarded equation of motion, but exist also in the LLG equation with very small damping; the oscillations are suppressed by the dissipation field in the LLG equation, whereas the dissipation field is of the same origin as the effective field in the time-retarded equation of motion (3).

At variance with the findings in Ref. [42], we find here that the trajectory is a curtate cycloid; a prolate cycloid was not observed for time retardation.

The approximate analytical result of Eq. (13) have been further analyzed by numerical simulations which we report on now. We address, in particular, the dependence of the precession frequency ω, the nutation frequency ω_n, and the damping rate R on Γ_1 and on τ_s (shown in Fig. 3). Since the value of the macrospin is only a linear scaling parameter, we set $m_\mathrm{s} = 1\,\mu_\mathrm{B}$.

Both the amplitude Γ_1 as well as the retardation time τ_s determine the damping (black lines in Fig. 3). τ_s produces an exponential slope corresponding to $\Delta R = 4.38$, whereas Γ_1 leads to $\Delta R = 1.98$. This suggests that τ_s dominates the damping compared to Γ_1. In addition, the precession frequency ω and the nutation frequency ω_n depend linearly on both parameters (red lines in Fig. 3), in agreement with the analytical calculations (13), assuming $\omega\tau_\mathrm{s} = \mathrm{const}$. The nutation amplitude, however, does not depend on Γ_1/Γ_0; it is of the order of $1.73 \times 10^{-2}\,\mu_\mathrm{B}$ (the error of the nutation amplitude at different times is in the range of $1 \times 10^{-6}\,\mu_\mathrm{B}$).

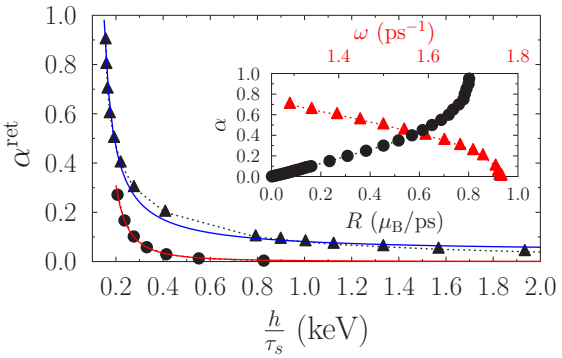

FIG. 4. (Color online) Mapping of the retardation energy $\Sigma_s = h\tau_s^{-1}$ and the Gilbert damping constant α for the "exponential" retardation kernel (circles, $\Gamma_1 = 0.5\Gamma_0$) and the Gaussian retardation kernel (triangles, $\Gamma_0 = 1$ as). The data are fitted by a Lorentzian (red line) for $\mathbf{\Gamma}^{\rm exp}$ and by $1/\Sigma_s$ (blue line) for $\mathbf{\Gamma}^{\rm Gauss}$. Inset: α vs relaxation rate R (black circles) as well as α vs the characteristic precession frequency ω (red triangles) for the conventional equation of motion. Lines are a guide to the eye.

Since the correlation time τ_s dominates the damping, a relation between τ_s and $\alpha^{\rm ret}$ is desirable. To achieve such a mapping (shown in Fig. 4), we solved the nonretarded equation of motion for various Gilbert damping parameters; subsequently, the damping rates R obtained from both equations are compared. The inset of Fig. 4 shows the increase of the Gilbert damping α with damping rate R in the conventional LLG equation. At high damping, the magnetic moment relaxes within one precession cycle toward the direction of the external field (Fig. 4 provides the characteristic frequencies with respect to the damping calculated from the first two oscillation maxima.).

The Gilbert-like damping constant $\alpha^{\rm ret}$ introduced by time retardation (Fig. 4) is inversely proportional to the squared retardation energy $\Sigma_s = \hbar/\tau_s$ and can be fitted nicely by a Lorentzian (red line in Fig. 4). This fit strongly supports the relation between the Gilbert damping and the relaxation time which is established by the Kamberský theory, as discussed by Gilmore *et al.* [9]. Furthermore, the width of the Lorentzian scales linearly with Γ_1/Γ_0 and the magnetocrystalline anisotropy.

To conclude this section, we briefly address the Gaussian retardation kernel of Eq. (8). The analytical solution for the retarded field is expressed in terms of error functions (not shown here). It turns out that this kernel significantly increases the slope ΔR for τ_s. The mapping $\alpha^{\rm ret}$ versus τ_s (triangles in Fig. 4) illustrates that the retarded damping α as well as the damping rate R scale linearly with τ_s for the chosen strength of $\Gamma_0 = 1$ as. Unphysically large Γ_0 or anisotropies K produce higher orders in τ_s, as will be discussed in Sec. III B.

For a macrospin, we conclude that sufficiently large retardation times and correlation strengths cause Gilbert-like damping and magnetic inertia. Both retardation kernels yield the same trend: the stronger the retardation energy Σ_s, the lower the damping, which is similar to phonon-mediated damping [10,11].

B. Exchange-coupled systems: Bulk Fe and Co

For exchange-coupled systems, the dynamics of the magnetic moments becomes more complex. In the following, we address bulk bcc Fe and hcp Co with the aim to study the damping caused by the Heisenberg exchange. Considering the easy axis of the magnetocrystalline anisotropy to be oriented along the $+z$ direction for both bcc Fe and hcp Co [44], which in our studies coincides with the direction of the external magnetic field, one can say that magnetic anisotropy will provide a contribution similar to that of the external field, especially due to the fact that both quantities (anisotropy field and external field) are of comparable magnitude. However, as we are considering an atomistic approach with small size of the modeled clusters, the fields associated with the exchange coupling will strongly dominate both the magnetocrystalline anisotropy field and the applied field. Under these circumstances, it is reasonable to neglect the anisotropy term, which considerably simplifies the analytics by removing the quantum-mechanical magnetic effects, according to results published by Wieser *et al.*; see Refs. [37] and [38]. To ease the analysis, we restrict ourselves to a collinear initial configuration of magnetic moments, with the consequence that the magnetic structure can be viewed as a macrospin at any time t. We will show that correlation in time will generate larger damping due to the Heisenberg exchange. This suggests that even for a collinear configuration, the internal constituents are important.

In a collinear magnetic state, the exchange field $\boldsymbol{B}^{\rm ex}(t)$ at time t does not contribute to the evolution of the magnetic moments [red arrow in Fig. 5(b)]. However, at time t', it causes, due to the time retardation, a field not necessarily parallel to the magnetic moments at time t [cf. the orange arrows in Figs. 5(b) and 5(c)]. This field can be decomposed into a moving tripod [Fig. 5(a)] which consists of a component parallel to the effective field $\boldsymbol{B}$ at time t, a component parallel to the dissipation field $\boldsymbol{B}^{\rm diss} \propto {}^{\partial \boldsymbol{m}}/_{\partial t}$ at time t, and an inertialike component $\boldsymbol{B}^{\rm in}$:

$$\begin{aligned}\boldsymbol{B}^{\rm ret} &= \boldsymbol{B} + \boldsymbol{B}^{\rm diss} + \boldsymbol{B}^{\rm in} \\ &= (\boldsymbol{B}^{\rm ret}\cdot\boldsymbol{e})\boldsymbol{e} + (\boldsymbol{B}^{\rm ret}\cdot\boldsymbol{e}^{\rm diss})\boldsymbol{e}^{\rm diss} + \boldsymbol{B}^{\rm in}. \end{aligned} \tag{15}$$

Here, $\boldsymbol{e}$ and $\boldsymbol{e}^{\rm diss}$ are the directions of the effective and the dissipation field at time t, respectively. This decomposition is obtained analytically by integrating the Heisenberg exchange convolution field [first term in Eq. (9)], assuming nearest-neighbor interactions J and a small retarded damping α. Consequently, the Cartesian components of a magnetic moment can be represented by sine and cosine functions, as in Eq. (12) of Sec. III A.

For the retardation kernel in Eq. (6), the retardation field reads

$$\begin{aligned}\boldsymbol{B}^{\rm ret}(t) &= 2NJ\int_0^t \mathbf{\Gamma}^{\rm exp}(t-t')\,\boldsymbol{m}(t')dt' \\ &= \frac{2NJ\Gamma_1\tau_s}{\omega^2\tau_s^2+1}\left(\boldsymbol{m} - \tau_s\frac{\partial \boldsymbol{m}}{\partial t} + \boldsymbol{c}^{\rm in}\right) \end{aligned} \tag{16}$$

(N coordination number). The functional form of $\boldsymbol{B}^{\rm ret}$ is similar to that for a macrospin [Eq. (13)], however, without projection to a specific direction. Thus, the retarded damping

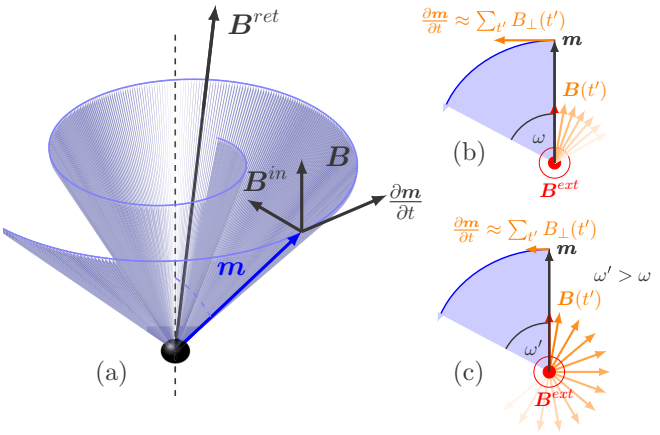

FIG. 5. (Color online) Evolution of a magnetic moment in an exchange-coupled system under the influence of time retardation (schematic). (a) Decomposition of the retardation field into a moving tripod consisting of the effective field $\boldsymbol{B}$ at time t, the damping field $\partial \boldsymbol{m}/\partial t$, and the inertia field $\boldsymbol{B}^{\text{in}}$. (b) Trajectory of the magnetic moment based on the equation of motion with time retardation. The moment precesses with the frequency ω, which is determined by the strength of the external field $\boldsymbol{B}^{\text{ext}}$. The retarded damping is caused by the fields $\boldsymbol{B}(t')$ at time t' (orange arrows), leading to the dissipation field $\sum_{t'} B_\perp(t')$. (c) If the field is in the direction of $\boldsymbol{B}^{\text{ext}}$ and the precession frequency ω' ($\omega' > \omega$) increases due to the retardation, the retarded damping and the retarded field $\boldsymbol{B}^{\text{ret}}$ parallel to the magnetic moment decrease, which destabilizes the dynamics of the magnetic moment.

is always positive definite, which is corroborated by numerical simulations.

It follows from Eq. (16) that the retarded damping as well as the inertia are frequency dependent, in accordance with the Cummins equation (5). This dependence is controlled by the Heisenberg exchange and is illustrated as follows. The exchange field at time t in the collinear state is parallel to the average magnetic moment $\boldsymbol{M} = \sum_i \boldsymbol{m}_i$ at t; more precisely, in the nearest-neighbor model of Eq. (16), the exchange field reads $\boldsymbol{B}^{\text{ex}} = J\boldsymbol{M}$. This exchange field can always be decomposed into a field parallel ($\boldsymbol{B}_\parallel$) and perpendicular ($\boldsymbol{B}_\perp$) to the external magnetic field. $\boldsymbol{B}_\perp$ comprises the damping and inertia fields of Eq. (15). Since the average magnetic moment will equilibrate in the direction of the external magnetic field, $\boldsymbol{B}_\parallel$ increases, whereas $\boldsymbol{B}_\perp$ decreases. We recall that the torque $\boldsymbol{m}(t) \times \boldsymbol{B}^{\text{ex}}(t)$ is zero in a coherent magnetic state.

With retardation, however, the torque $\boldsymbol{m}(t) \times \boldsymbol{B}^{\text{ex}}(t')$ is nonzero since, in nonequilibrium, magnetic moments at different times point in different directions. Decomposing the exchange field at t' reveals that $\boldsymbol{B}_\parallel(t')$ contributes effectively to the external field due to the retardation and, consequently, leads to higher precession frequencies ω, in accordance with the Larmor law [Fig. 5(c)]. Hence, the product $\omega\tau_s$—the number of oscillations within the fixed time interval τ_s—increases. In contrast, $\boldsymbol{B}_\perp(t')$ and $\boldsymbol{B}_\perp(t'')$ decrease in time and may be aligned antiparallel to each other for sufficiently large ω and fixed τ_s [orange arrows in Fig. 5(c)]. Since $\boldsymbol{B}_\perp(t'')$ is larger than $\boldsymbol{B}_\perp(t')$ for $t'' < t'$, the retarded damping—which is proportional to $\boldsymbol{B}_\perp$—could be reduced or even vanish. In contrast, a small ω always leads to an enhanced retarded

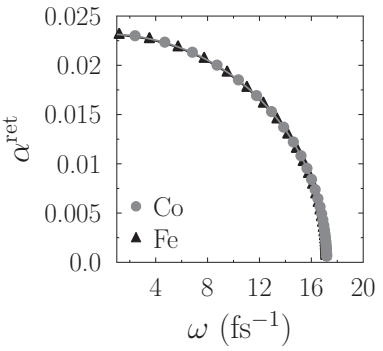

FIG. 6. Retarded damping α^{ret} vs precession frequency ω of the retardation field $\boldsymbol{B}_\parallel$ per atom for Fe (black triangles) and Co (gray circles); $\Gamma_1 = 0.05\Gamma_0$ and $\tau_s = 3$ as. Lines are added to guide the eye.

damping. Consequently, the damping decreases or oscillates with frequency (Fig. 6).

This decrease depends on both the Heisenberg exchange parameter and the correlation time τ_s. For small τ_s (Fig. 6), material-specific differences in the retarded damping are small (cf. Fig. 8); thus, the tuning of α^{ret} with the frequency ω is very similar in Fe and Co. We recall that ω is specified by the exchange field and, therefore, cannot be probed by ferromagnetic resonance measurements operating in the GHz regime.

The inertia field $\boldsymbol{B}^{\text{in}} = {}^{2NJ\Gamma_1\tau_s}/_{(\omega^2\tau_s^2+1)}\,\boldsymbol{c}^{\text{in}}$ tilts the moment out of the equilibrium direction, and the solution of the equation of motion becomes unstable. Thus, in what follows, $\boldsymbol{c}^{\text{in}}$ has to be neglected, in accordance with Ref. [45] which exemplifies negligible inertia in bulk materials; nutation cycloids were revealed at the edges of low-dimensional magnets, where less coordination in the Heisenberg exchange could cause magnetic inertia. Furthermore, Ref. [25] postulates important magnetic inertia for narrow-band magnetic materials, such as strongly correlated electron systems, and noncollinear magnetic states. Both arguments do not apply for the collinear Stoner magnets examined in this paper.

We now address the dependence of the damping rate R on the nearest-neighbor exchange, the retardation strength Γ_1, as well as the retardation time τ_s for hcp Co and bcc Fe (Fig. 7).

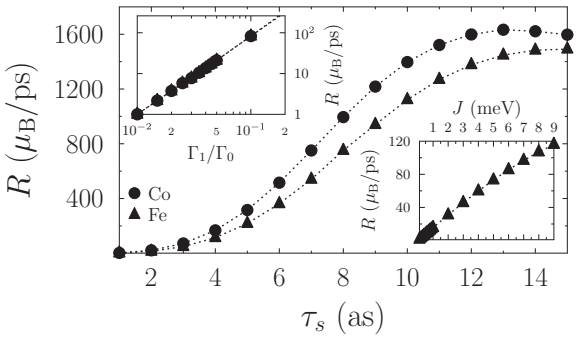

FIG. 7. Damping rate R vs correlation time τ_s for bulk Fe (triangles) and Co (circles); $\Gamma_1 = 0.2\Gamma_0$. The top-left inset shows R vs retardation strength ${}^{\Gamma_1}/_{\Gamma_0}$ for $\tau = 5$ as, whereas the bottom-right inset depicts R vs the nearest-neighbor exchange J for a bcc structure. Lines are added to guide the eye.

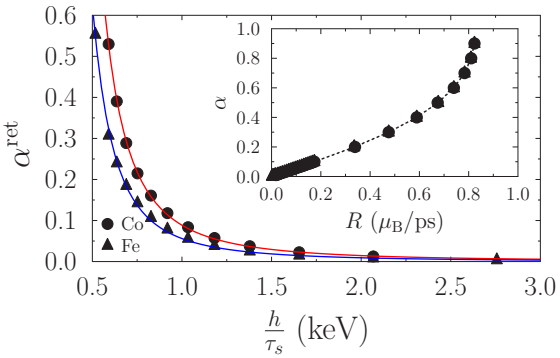

FIG. 8. (Color online) Mapping of the retarded damping constant $\alpha^{\rm ret}$ and the retardation time τ_s for bulk Fe (triangles and blue line) and Co (circles and red line); $\Gamma_1 = 5 \times 10^{-3}\Gamma_0$. The data are fitted by a Lorentzian. Inset: The Gilbert damping α vs damping rate R obtained from the conventional LLG equation.

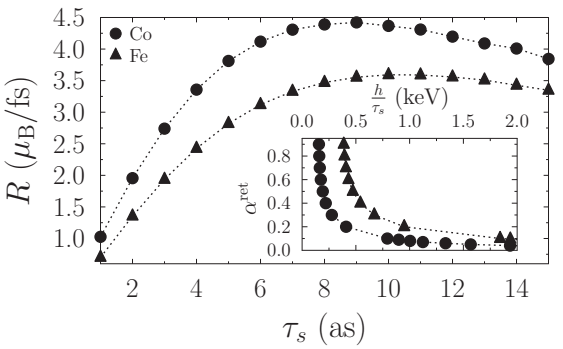

FIG. 9. Damping rate R vs retardation time τ_s for bulk Fe (triangles) and Co (circles) for the Gaussian retardation kernel with $\Gamma_0 = 1\,\text{as}^{-1}$. Inset: The mapping of the retarded damping constant $\alpha^{\rm ret}$ and the correlation time τ_s for $\Gamma_0 = 1\,\text{fs}^{-1}$. Lines are added to guide the eye. Please note that the abscissa label of the inset is on top of the figure.

The linear proportionality of R with respect to the Heisenberg exchange J is valid only for very small J (we recall that the nearest-neighbor J for bulk Fe is 12.77 meV, as obtained from electronic structure calculations [45,46]). For larger J, the damping increases dramatically and higher-order terms have to be taken into account. By successively increasing the Heisenberg interaction to higher neighbor shells (not shown here), the damping rate can increase or decrease, which is attributed to the sign of the J_{0j}'s that are associated with the neighbor shells (j) [45]. The damping rate of hcp Co is larger than that of bcc Fe due to the stronger exchange (bulk Co: $J = 13.56$ meV; second-nearest-neighbor J's are 11.31 meV for Fe and 12.08 meV for Co, respectively [45]). This finding is in accordance with the Kamberský model discussed in Refs. [9] and [14].

Since the Heisenberg exchange is larger than the anisotropy, a τ_s smaller than for a macrospin situation would yield the same damping rate R. R increases exponentially with τ_s, but saturates at $\tau_s > 12$ as. This is explained by a damping faster than one period of precession. For even higher τ_s, the rate decreases, which is mediated by the aforementioned frequency dependence of the damping. The position of the inflection point shifts with the Heisenberg exchange and the correlation strength; it scales quadratically with the latter.

As for the macrospin, we map the retarded damping $\alpha^{\rm ret}$ and τ_s (Fig. 8). We obtain a Lorentzian-like decrease of the damping with the retardation energy $\Sigma_s = \hbar/\tau_s$. The Heisenberg exchange generates a higher damping for the same τ_s than for the macrospin model; likewise, the damping for Co is larger than for Fe. The damping rate R from the LLG equation, however, for both ferromagnets is almost identical (inset in Fig. 8) since the Heisenberg interactions do not contribute to the torque.

Finally, we briefly address the Gaussian retardation kernel (Fig. 8). The dependence of the damping rate R on the correlation time τ_s differs from that obtained for the exponential retardation kernel. Direct proportionality between R and τ_s shows up for small values, whereas larger values yield a maximum and subsequent decrease to $\exp(-\tau_s^2\omega^2/4)$. The slope and the position of the maximum depend on the strength of the magnetic exchange and the correlation: the larger J and Γ_1/Γ_0, the smaller the correlation τ_s. Assuming a linear relation between R and τ_s, one finds a one-to-one correspondence of the retarded dissipation and the correlation time (inset in Fig. 9).

In conclusion, we find that—although we consider a collinear state of the atomic magnetic moments which can be viewed as a macrospin—it is important to account for the Heisenberg exchange within an assembly of magnetic moments. The latter is responsible for a significant contribution to the damping in Fe and Co, which is due to the retardation.

To check relaxations in a noncollinear case, we also applied our model to 2 ML Co nanoislands on Cu(111) (not shown here), with exchange parameters taken from Ref. [47]. An atomic magnetic moment at the rim of an island has a smaller coordination N [cf. Eq. (16)] compared to sites in the center. Thus, the retardation field causes a retarded damping at the rim which differs from that at an island's center, as is expected for low-dimensional systems within the Kamberský model [14].

IV. CONCLUDING REMARKS

In this paper, we present and discuss an *ansatz* for the time-retarded equation of motion for atomistic magnetization dynamics, with a focus on damping. For various examples, a connection between the correlation time τ_s—that is, the duration in which a magnetic moment "is aware of" its history—and the Gilbert damping constant α. In particular, we show that the mapping of both quantities depends on the correlation strength, the chosen retardation kernel, and the intrinsic magnetic parameters, such as Heisenberg exchange and magnetocrystalline anisotropy. Thus, time retardation is a damping mechanism in addition to well-established mechanisms, e.g., damping mediated by electron-phonon coupling. The results are consistent with the works of Kamberský [48] and Bose *et al.* [24].

The relations deduced in the present work are applicable also for low-dimensional magnetic systems. Due to reduced coordination, for example at a surface, the effective exchange and, therefore, the damping become site dependent. Numerical simulations (not shown here) establish that the damping at

a surface can be sufficiently large to maintain a collinear magnetic configuration.

Considering future investigations, we would like to emphasize that the retardation mechanism is not able to describe damping in a thermal bath since the retarded field vanishes in this case. This implies that the thermal energy cannot dissipate to the same reservoir or—in the sense of time retardation—from time t to t' (where $t' < t$). Thus, the coupling to other reservoirs (Fig. 1) and other damping mechanisms are essential. Another open question concerns the inertia field, which in some cases destabilizes the system. Studies of these phenomena are underway.

ACKNOWLEDGMENTS

The support of the Swedish Research Council (VR), eSSENCE, and the Knut and Allice Wallenberg foundation is acknowledged.

[1] R. O. Cherifi, V. Ivanovskaya, L. C. Phillips, A. Zobelli, I. C. Infante, E. Jacquet, V. Garcia, S. Fusil, P. R. Briddon, N. Guiblin *et al.*, Nat. Mater. **13**, 345-351 (2014).
[2] Y. Kato, R. C. Myers, A. C. Gossard, and D. D. Awschalom, Nature (London) **427**, 50 (2004).
[3] S. Salahuddin, Ph.D. thesis, Purdue University, 2007.
[4] S. Yan, Ph.D. thesis, University of South Carolina, 2014.
[5] S. Heinze, K. von Bergmann, M. Menzel, J. Brede, A. Kubetzka, R. Wiesendanger, G. Bihlmayer, and S. Blügel, Nature (London) **7**, 713-718 (2011).
[6] N. Okamoto, H. Kurebayashi, T. Trypiniotis, I. Farrer, D. A. Ritchie, E. Saitoh, J. Sinova, J. Maŝek, and C. H. W. Jungwirth, and T. Barnes, Nature (London) **13**, 932-937 (2014).
[7] T. L. Gilbert, IEEE Trans. Magn. **40**, 6 (2004).
[8] V. Kamberský, Can. J. Phys. **48**, 2906 (1970).
[9] K. Gilmore, Y. U. Idzerda, and M. D. Stiles, Phys. Rev. Lett. **99**, 027204 (2007).
[10] H. Ebert, S. Mankovsky, D. Ködderitzsch, and P. J. Kelly, Phys. Rev. Lett. **107**, 066603 (2011).
[11] S. Mankovsky, D. Ködderitzsch, G. Woltersdorf, and H. Ebert, Phys. Rev. B **87**, 014430 (2013).
[12] D. Steiauf and M. Fähnle, Phys. Rev. B **72**, 064450 (2005).
[13] M. Fähnle and D. Steiauf, Phys. Rev. B **73**, 184427 (2006).
[14] D. Thonig and J. Henk, New J. Phys. **16**, 013032 (2014).
[15] A. Brataas, Y. Tserkovnyak, and G. E. W. Bauer, Phys. Rev. B **84**, 054416 (2011).
[16] Y. Wang, W.-Q. Chen, and F.-C. Zhang, New J. Phys. **17**, 053012 (2015).
[17] P. Pirro, T. Sebastian, T. Brächer, A. A. Serga, T. Kubota, H. Naganuma, M. Oogane, Y. Ando, and B. Hillebrands, Phys. Rev. Lett. **113**, 227601 (2014).
[18] C. Schütte and M. Garst, Phys. Rev. B **90**, 094423 (2014).
[19] J. Iwasaki, A. J. Beekman, and N. Nagaosa, Phys. Rev. B **89**, 064412 (2014).
[20] T. Weindler, H. G. Bauer, R. Islinger, B. Boehm, J.-Y. Chauleau, and C. H. Back, Phys. Rev. Lett. **113**, 237204 (2014).
[21] T. Bose, Ph.D. thesis, Martin Luther University, Halle/Wittenberg, 2013.
[22] H. T. Nembach, J. M. Shaw, C. T. Boone, and T. J. Silva, Phys. Rev. Lett. **110**, 117201 (2013).
[23] T. Bose and S. Trimper, Phys. Rev. B **81**, 104413 (2010).
[24] T. Bose and S. Trimper, Phys. Rev. B **83**, 134434 (2011).
[25] S. Bhattacharjee, L. Nordström, and J. Fransson, Phys. Rev. Lett. **108**, 057204 (2012).
[26] A. Naess and T. Moan, *Stochastic Dynamics of Marine Structures* (Cambridge University Press, Cambridge, 2013).
[27] M.-C. Ciornei, Ph.D. thesis, Ecole Polytechnique, Universidad de Barcelona, 2010.
[28] M.-C. Ciornei, J. M. Rubí, and J.-E. Wegrowe, Phys. Rev. B **83**, 020410 (2011).
[29] A. I. Lichtenstein and M. I. Katsnelson, Phys. Rev. B **57**, 6884 (1998).
[30] P. Weinberger, *Electron Scattering Theory of Ordered and Disordered Matter* (Clarendon, Oxford, 1990).
[31] *Electron Scattering in Solid Matter*, edited by J. Zabloudil, R. Hammerling, L. Szunyogh, and P. Weinberger (Springer, Berlin, 2005).
[32] L. Bergqvist, A. Taroni, A. Bergman, C. Etz, and O. Eriksson, Phys. Rev. B **87**, 144401 (2013).
[33] N. Leo, A. Bergman, A. Cano, N. Poudel, B. Lorenz, M. Fiebig, and D. Meier, Nat. Commun. **6**, 6661 (2015).
[34] A. Bergman, B. Skubic, J. Hellsvik, L. Nordström, A. Delin, and O. Eriksson, Phys. Rev. B **83**, 224429 (2011).
[35] B. Skubic, Ph.D. thesis, Uppsala Universitet, 2007.
[36] V. P. Antropov, M. I. Katsnelson, B. N. Harmon, M. van Schilfgaarde, and D. Kusnezov, Phys. Rev. B **54**, 1019 (1996).
[37] R. Wieser, Phys. Rev. B **84**, 054411 (2011).
[38] R. Wieser, Phys. Rev. Lett. **110**, 147201 (2013).
[39] J. H. Mentink, M. V. Tretyakov, A. Fasolino, M. I. Katsnelson, and T. Rasing, J. Phys.: Condens. Matt. **22**, 176001 (2010).
[40] R. B. Leighton, Rev. Mod. Phys. **20**, 165 (1948).
[41] R. L. S. Farias, R. O. Ramos, and L. A. da Silva, Phys. Rev. E **80**, 031143 (2009).
[42] D. Böttcher and J. Henk, Phys. Rev. B **86**, 020404 (2012).
[43] E. C. Stoner and E. P. Wohlfarth, Philos. Trans. R. Soc. London A **240**, 599 (1948).
[44] G. H. O. Daalderop, P. J. Kelly, and M. F. H. Schuurmans, Phys. Rev. B **41**, 11919 (1990).
[45] D. Böttcher, A. Ernst, and J. Henk, J. Magn. Magn. Mater. **324**, 610 (2012).
[46] M. Pajda, J. Kudrnovský, I. Turek, V. Drchal, and P. Bruno, Phys. Rev. B **64**, 174402 (2001).
[47] D. Böttcher, A. Ernst, and J. Henk, J. Phys.: Condens. Matt. **23**, 29 (2011).
[48] V. Kamberský, Czech. J. Phys. B **34**, 1111 (1984).